Temporal changes in Hec1 phosphorylation control kinetochore–microtubule attachment stability during mitosis

Keith F. DeLuca[1], Susanne M. A. Lens[2] and Jennifer G. DeLuca[1,*]

[1]Department of Biochemistry and Molecular Biology, Colorado State University, Fort Collins, CO 80523, USA
[2]Laboratory of Experimental Oncology, Department of Medical Oncology, University Medical Center Utrecht, Stratenum 2.125, Universiteitsweg 100, 3584 CG Utrecht, The Netherlands
*Author for correspondence (jdeluca@colostate.edu)

Accepted 21 October 2010
Journal of Cell Science 124, 622-634

doi:10.1242/jcs.072629

Summary

Precise control of the attachment strength between kinetochores and spindle microtubules is essential to preserve genomic stability. Aurora B kinase has been implicated in regulating the stability of kinetochore–microtubule attachments but its relevant kinetochore targets in cells remain unclear. Here, we identify multiple serine residues within the N-terminus of the kinetochore protein Hec1 that are phosphorylated in an Aurora-B-kinase-dependent manner during mitosis. On all identified target sites, Hec1 phosphorylation at kinetochores is high in early mitosis and decreases significantly as chromosomes bi-orient. Furthermore, once dephosphorylated, Hec1 is not highly rephosphorylated in response to loss of kinetochore–microtubule attachment or tension. We find that a subpopulation of Aurora B kinase remains localized at the outer kinetochore even upon Hec1 dephosphorylation, suggesting that Hec1 phosphorylation by Aurora B might not be regulated wholly by spatial positioning of the kinase. Our results define a role for Hec1 phosphorylation in kinetochore–microtubule destabilization and error correction in early mitosis and for Hec1 dephosphorylation in maintaining stable attachments in late mitosis.

Key words: Kinetochore, NDC80, Hec1, Microtubule, Aurora B

Introduction

At the onset of mitosis, bipolar spindle formation and initial microtubule (MT) capture by kinetochores occur simultaneously, which inevitably results in the formation of many erroneous kinetochore–MT attachments (reviewed by Vader et al., 2008; Cimini, 2008). If left uncorrected, attachment errors can be detrimental to the resulting daughter cells. For example, if anaphase is initiated in cells containing syntelic attachments, in which two sister kinetochores of a mitotic chromosome are attached to MTs from one pole, both sister chromatids of the chromosome will distribute into one daughter cell, resulting in the formation of two aneuploid cells. In the case of uncorrected merotelic attachments, in which one kinetochore is attached to MTs from both spindle poles, the cell might or might not correctly distribute the sister chromatids, depending on the outcome of a tug-of-war between bundles of MTs from opposite poles (Cimini et al., 2004). Thus, it is crucial in early mitosis, when attachment errors are frequently made, that kinetochore–MTs are labile to prevent the accumulation of erroneous attachments. It is equally important, however, that kinetochore–MT attachments are stabilized following bi-orientation so that sustained forces can be generated for chromosome movement and to silence the spindle assembly checkpoint.

The chromosomal passenger complex, comprising Aurora B kinase, INCENP, Survivin and Borealin, has been implicated in kinetochore–MT error correction during mitosis (reviewed by Vader et al., 2008). Inhibition of Aurora B kinase results in an increase in syntelic and merotelic attachments in cultured cells (Ditchfield et al., 2003; Hauf et al., 2003; Lampson and Kapoor, 2005; Cimini et al., 2006; Knowleton et al., 2006), and decreased Aurora B kinase activity leads to hyper-stable kinetochore–MTs (Cimini et al., 2006). Furthermore, the budding yeast Aurora kinase homolog Ipl1 has been shown to induce kinetochore–MT detachment in response to decreased tension (Pinsky et al., 2006; Biggins and Murray, 2001; Tanaka et al., 2002). Together, these results suggest that Aurora B kinase promotes detachment of incorrectly attached MTs by reducing the stability of kinetochore–MTs.

In vitro, Aurora B kinase phosphorylates the kinetochore-associated NDC80 complex component Hec1 (Cheeseman et al., 2002; DeLuca et al., 2006; Ciferri et al., 2008), and the two proteins have been shown to interact through co-immunoprecipitation experiments (Tien et al., 2004). The NDC80 complex is required for generating stable, end-on kinetochore–MT attachments (Wigge and Kilmartin, 2001; DeLuca et al., 2002; Martin-Lluesma et al., 2002; McCleland et al., 2004) and has been suggested to provide a direct linkage between kinetochores and the MT lattice in higher eukaryotes (Cheeseman et al., 2006; Wei et al., 2007; Ciferri et al., 2008). Expression in PtK1 cells of a Hec1 mutant in which six Aurora B kinase target sites (identified from in vitro studies) were mutated to alanine (Ala) to prevent phosphorylation resulted in stable kinetochore–MT attachments, but an increase in kinetochore–MT attachment errors (DeLuca et al., 2006). Furthermore, inclusion of purified Aurora B kinase in MT co-sedimentation assays resulted in decreased binding affinity of the NDC80 complex for MTs (Cheeseman et al., 2006; Ciferri et al., 2008). These results suggest that phosphorylation of Hec1 by Aurora B kinase in cells might reduce the affinity of kinetochores for MTs, leading to kinetochore–MT release. However, it remains unknown whether Hec1 is a substrate of Aurora B kinase in vivo

Journal of Cell Science

or if phosphorylation is physiologically relevant to kinetochore–MT stability. Using phosphorylation-specific antibodies generated to residues in the N-terminal tail domain of Hec1, we demonstrate that multiple target sites are phosphorylated in an Aurora-B-kinase-dependent manner. Each of these sites is highly phosphorylated in early mitosis and phosphorylation significantly decreases as chromosomes bi-orient. Our findings suggest that the N-terminus of Hec1, through phosphorylation and dephosphorylation, regulates kinetochore–MT stability to facilitate error correction in early mitosis and chromosome bi-orientation and silencing of the spindle assembly checkpoint in late mitosis.

Results

Phosphorylation of the Hec1 N-terminus regulates kinetochore–MT stability and dynamics

To investigate the role for Hec1 tail phosphorylation in kinetochore–MT stability, we first depleted endogenous Hec1 from PtK1 cells and subsequently rescued the depletion by transfecting cells with constructs encoding for either human wild-type (WT)-Hec1–GFP or 9A-Hec1–GFP, in which all nine putative Aurora B kinase target phosphorylation sites within the unstructured N-terminal tail domain (Ser4, Ser5, Ser8, Ser15, Ser44, Thr49, Ser55, Ser62 and Ser69) were mutated to Ala to prevent phosphorylation (DeLuca et al., 2006; Ciferri et al., 2008; Guimaraes et al., 2008). Consistent with overexpression studies (DeLuca et al., 2006), cells rescued with the 9A-Hec1–GFP mutant generated end-on kinetochore–MT attachments as efficiently as cells rescued with WT-Hec1–GFP (Fig. 1A,B). Additionally, kinetochores in cells rescued with 9A-Hec1–GFP were able to generate inter-kinetochore tension, as reflected by inter-kinetochore distance measurements (Fig. 1C). Cells rescued with 9A-Hec1–GFP did, however, exhibit chromosome alignment defects, in which few cells were capable of aligning all chromosomes at the spindle equator (Fig. 1D). Specifically, many 9A-Hec1–GFP-rescued cells generated partial metaphase plates, in which some chromosomes were unable to align and remained close to one pole with both sister kinetochores attached to microtubules (Fig. 1A). HeLa cells depleted of endogenous Hec1 and rescued with 9A-Hec1–GFP exhibited similar phenotypes. Specifically, some cells were able to congress their chromosomes to the spindle equator, but a significant portion exhibited a prometaphase-like phenotype or contained partial metaphase plates with multiple chromosomes stranded at one or both spindle poles (Fig. 1E). Inter-kinetochore distance measurements indicated that bi-oriented sister kinetochores in HeLa cells rescued with 9A-Hec1–GFP were able to generate inter-kinetochore tension (Fig. 1F). These results indicate that prevention of Hec1 phosphorylation results in stable kinetochore-microtubule attachments and defects in chromosome alignment.

To determine whether the phenotypes observed in cells rescued with 9A-Hec1–GFP were due to hyper-stable kinetochore–MT attachments, we performed a monastrol washout experiment. Treatment of a cell population with the small-molecule Eg5-inhibitor monastrol results in the accumulation of cells with monopolar spindles (Mayer et al., 1999), and a consequence of this is the formation of many syntelically attached sister kinetochore pairs (Kapoor et al., 2000). After drug washout, monopolar spindles are quickly converted to bipolar spindles, and syntelic attachments are replaced with amphitelic attachments (Kapoor et al., 2000). Cells that are defective in releasing kinetochore–MT attachments correct syntelic attachments less efficiently and, as a result, bipolar spindle conversion is delayed and, upon bipolar spindle assembly, chromosome alignment is perturbed. HeLa cells rescued with 9A-Hec1–GFP exhibited a delay in bipolar spindle formation after monastrol washout when compared with cells rescued with WT-Hec1–GFP. After 1 hour, 98% of cells rescued with WT-Hec1–GFP had formed bipolar spindles, compared with 50% of cells rescued with 9A-Hec1–GFP (Fig. 1G,H). In addition, many cells rescued with 9A-Hec1–GFP converted monopolar spindles into multipolar spindles rather than directly forming bipolar spindles as in cells rescued with WT-Hec1–GFP. We next compared the phenotypes of WT- and 9A-Hec1–GFP-expressing cells with cells incubated in monastrol and washed out into media containing ZM447439, a potent Aurora B kinase inhibitor (Ditchfield et al., 2003). As expected, cells incubated with ZM447439 failed to efficiently form bipolar spindles after monastrol washout (Fig. 1G,H) and, at 60 minutes after washout initiation, only 40% of cells had bipolarized.

To address the role for Hec1 phosphorylation in kinetochore–MT plus-end assembly dynamics, we observed kinetochore movements in PtK1 cells depleted of endogenous Hec1 and rescued with WT-Hec1–GFP or 9A-Hec1–GFP. PtK1 cells rescued with WT-Hec1–GFP contained many bi-oriented sister kinetochore pairs that oscillated between the two spindle poles, as expected for control cells (Fig. 2A; supplementary material Movie 1). By contrast, oscillations of bi-oriented sister kinetochores in cells rescued with 9A-Hec1–GFP were dampened (Fig. 2A; supplementary material Movie 2). To quantify this, we tracked oscillations of bi-oriented sister kinetochore pairs in cells rescued with either WT-Hec1–GFP or 9A-Hec1–GFP (Fig. 2B). Indeed, as shown in Fig. 2C and 2D, the velocity of movement was decreased and the time spent in a ‘paused’ state was increased in kinetochores from cells rescued with 9A-Hec1–GFP compared with those from cells rescued with WT-Hec1–GFP. We also calculated the deviation from average position, which is a parameter developed by Wordeman and colleagues to gauge oscillation amplitude (Stumpff et al., 2008). This measurement is especially useful when it is difficult to determine the switch points, or changes in direction of movement, of oscillating kinetochores. The value for deviation from average position of kinetochores in 9A-Hec1–GFP rescued cells was significantly lower than for kinetochores in cells rescued with WT-Hec1–GFP (Fig. 2E), consistent with the qualitative observation that kinetochore oscillations were dampened in cells expressing mutant Hec1. Together, these results demonstrate that phosphorylation of the Hec1 tail domain during chromosome bi-orientation is required for normal plus-end kinetochore–MT stability and dynamics.

Multiple sites in the Hec1 N-terminus are phosphorylated in an Aurora-B-kinase-dependent manner

To determine which sites within the Hec1 N-terminus are phosphorylated in cells, we generated polyclonal antibodies specific to phosphorylated human Hec1 by immunizing rabbits with peptides containing phosphorylated amino acids previously shown to be targets of Aurora B kinase in vitro (DeLuca et al., 2006; Ciferri et al., 2008). Of the antibodies generated, those against Ser55-*P*, Ser44-*P*, Ser15-*P* and Ser8-*P* recognized kinetochores in cultured cells (Fig. 3A). Those against Ser55-*P*, Ser44-*P* and Ser8-*P* consistently recognized kinetochores in PtK1 cells (Fig. 3A), and kinetochore immunoreactivity, in all cases, was diminished in cells depleted of Hec1 by RNA interference (Fig. 3B; supplementary material Fig. S1). All antibodies recognized spindle poles as well as kinetochores; however, spindle pole localization was not

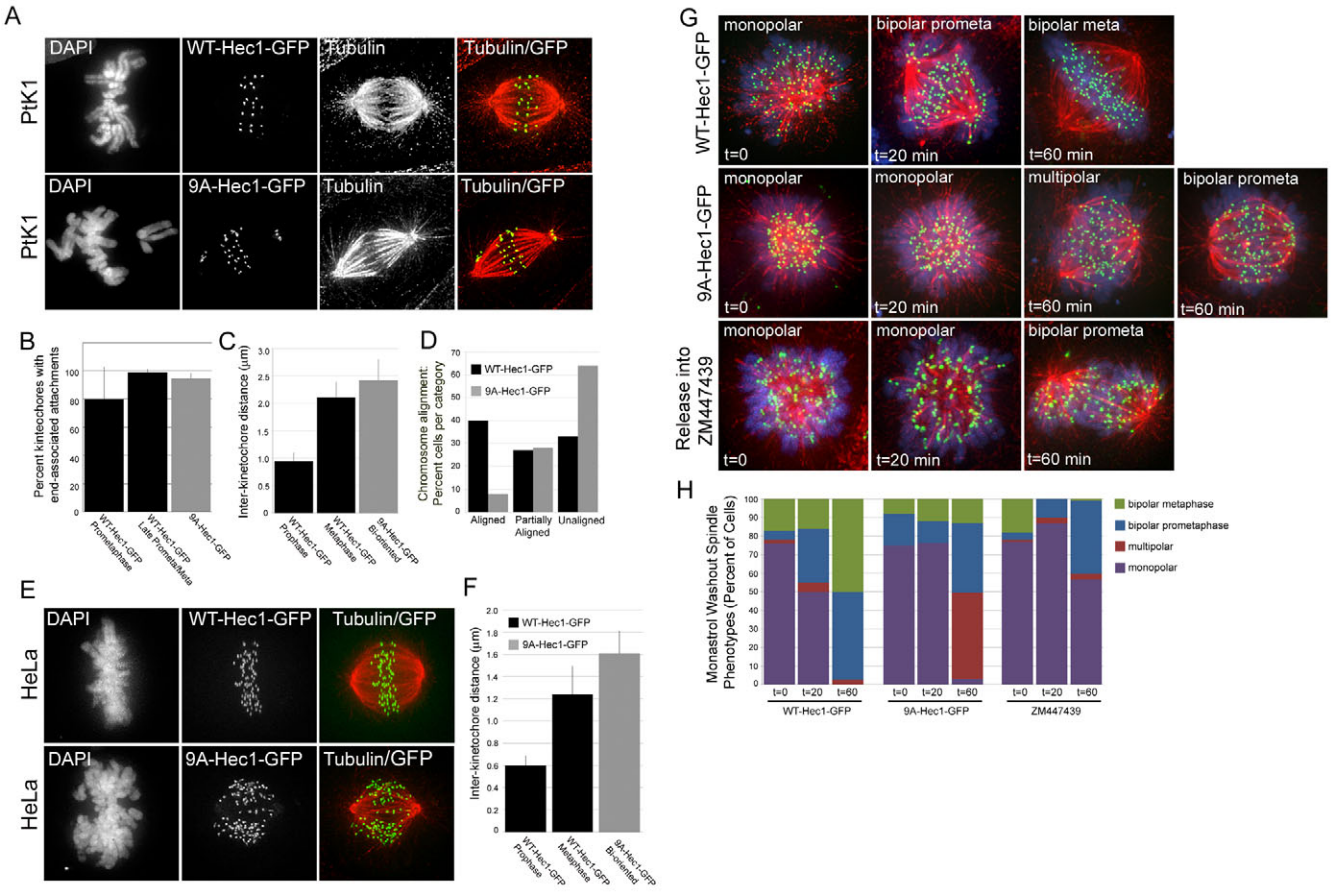

Fig. 1. Hec1 N-terminal phosphorylation is required for normal chromosome congression and regulation of kinetochore–MT attachments. (**A**) Immunofluorescence images of PtK1 cells depleted of endogenous Hec1 and rescued with either WT-Hec1–GFP or 9A-Hec1–GFP. (**B**) Quantification of end-on microtubule association with kinetochores (WT-Hec1–GFP prometaphase: *n*=448 kinetochores, 19 cells; WT-Hec1–GFP late prometaphase and metaphase: *n*=428 kinetochores, 14 cells; 9A-Hec1–GFP: *n*=247 kinetochores, 10 cells). (**C**) Quantification of inter-kinetochore distances in PtK1 cells. Distances between sister pairs were measured from GFP-centroid to GFP-centroid. For WT-Hec1–GFP rescued cells, measurements were taken from prophase and metaphase cells (*n*=45 kinetochore pairs, 10 cells and *n*=128 kinetochore pairs, 22 cells, respectively). For cells rescued with 9A-Hec1–GFP, inter-kinetochore distances were measured only from sister pairs of bi-oriented chromosomes (*n*=141 kinetochore pairs, 19 cells). (**D**) Quantification of chromosome alignment (*n*=161 cells for WT-Hec1–GFP; *n*=107 for 9A-Hec1–GFP). Cells containing less than 2 chromosomes off a well-defined metaphase plate were scored as having ‘aligned’ chromosomes. Cells containing 2–3 chromosomes off a metaphase plate were scored as having ‘partially aligned’ chromosomes. Cells exhibiting no discernible metaphase plate or those containing greater than 3 chromosomes off a metaphase plate were scored as having ‘unaligned’ chromosomes. (**E**) Immunofluorescence images of HeLa cells depleted of endogenous Hec1 and rescued with either WT-Hec1–GFP or 9A-Hec1–GFP. (**F**) Quantification of inter-kinetochore distances in HeLa cells. The *n* values are as follows: WT-Hec1–GFP metaphase, *n*=76 kinetochore pairs, 6 cells; WT-Hec1–GFP prophase, *n*=24 kinetochore pairs, 2 cells; 9A-Hec1–GFP (only kinetochores from bi-oriented chromosomes were scored), *n*=59 kinetochore pairs, 5 cells. (**G**) Immunofluorescence images of cells subjected to a monastrol washout assay. The top two rows show cells transfected with the GFP-fusion protein as indicated. Cells were treated with monastrol for 2 hours and then incubated in fresh culture media + MG132 for 1 hour. Samples of cells were subjected to immunofluorescence just prior to initiation of the monastrol washout, 20 minutes post-initiation of washout and 60 minutes post-initiation of washout. For the experiment in the bottom row, untransfected cells were treated with monastrol for 2 hours and then incubated in fresh media containing MG132 and 10 μM ZM447439. The predominant phenotypes at the indicated time-points are shown. Chromosomes are shown in blue, microtubules are shown in red and kinetochores are shown in green (GFP–Hec1 for the top two panels; ACA antibody staining in the bottom panel). (**H**) Quantification of monastrol washout experiment. For each condition, at least 75 cells were scored. Error bars indicate s.d.

significantly reduced in cells depleted of Hec1, suggesting that the kinetochore immunoreactivity was specific to the Hec1 protein (Fig. 3B; supplementary material Fig. S1). Although the anti-Ser15-*P* antibody recognized kinetochores in PtK1 cells, the staining was less consistent than that of the other antibodies; therefore, in PtK1 cells, we focused on the characterization of antibodies against Ser55-*P*, Ser44-*P* and Ser8-*P*. We tested the antibodies for immunoreactivity in HeLa and U2OS cells (Fig. 3A,B; supplementary material Figs S1 and S2) and found that those against Ser55-*P*, Ser44-*P* and Ser15-*P* recognized kinetochores in both cell types, whereas the anti-Ser8-*P* antibody did not recognize kinetochores consistently in either cell type. Similar to PtK1 cells, all antibodies recognized both kinetochores and spindle poles in HeLa cells, and cells depleted of Hec1 exhibited antibody localization at spindle poles but not at kinetochores (Fig. 3B; supplementary material Fig. S1). We next tested the phosphorylation-specificity of each antibody by carrying out in vitro kinase assays. Purified NDC80^{Bonsai}, a truncated version of the NDC80 complex deleted of much of its coiled-coil domain (Ciferri et al., 2008), was incubated with purified Aurora B kinase and a portion of its activator,

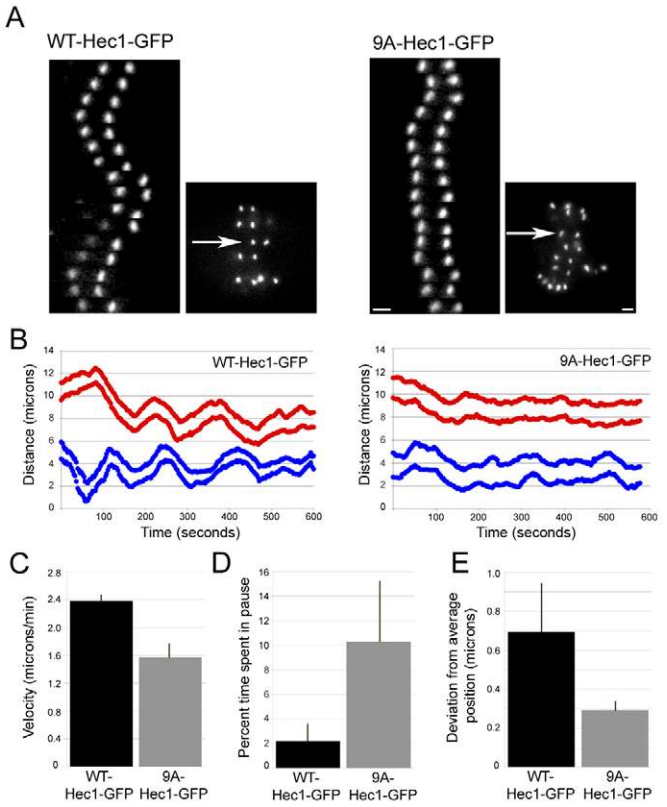

Fig. 2. Hec1 N-terminal phosphorylation is required for normal kinetochore oscillations. (**A**) Kymographs of a single sister kinetochore pair from live-cell time-lapse imaging sequences of PtK1 cells depleted of endogenous Hec1 and rescued with WT-Hec1–GFP (left) or 9A-Hec1–GFP (right). The arrows indicate which pairs are represented in the kymographs. (**B**) Plots indicating kinetochore oscillation movement over time. For each rescue experiment, two representative sister kinetochore pairs are shown. (**C**) Quantification of average velocity of kinetochore movement in rescued cells. Both pole-ward and away from the pole movements were measured (for graphs in C, D and E: WT-Hec1–GFP rescue, *n*=9 kinetochores, 4 cells; 9A-Hec1–GFP rescue, *n*=13 kinetochores, 4 cells). (**D**) Quantification of percent time in pause. If a kinetochore did not move for two sequential time points (6 seconds), a pause event was recorded. The percentage of time spent 'paused' was then calculated from the total time of the time-lapse image sequence. (**E**) Deviation from average position (Stumpff et al., 2008) was quantified for kinetochores in cells rescued with WT-Hec1–GFP and 9A Hec1–GFP kinetochores (see Materials and Methods). Scale bars: 2 µm. Error bars indicate s.d.

INCENP (Sessa et al., 2005), in the presence or absence of ATP. Whereas a non-phosphorylation-specific Hec1 antibody, termed 9G3 (Chen et al., 1997), recognized Hec1 of the NDC80^{Bonsai} complex in the presence and absence of ATP, the antibodies against Ser55-*P*, Ser44-*P*, Ser15-*P* and Ser8-*P* only recognized Hec1 in the presence of ATP (Fig. 3C), demonstrating that all four antibodies are specific for the phosphorylated form of Hec1. To determine if Aurora B kinase activity is required for Hec1 phosphorylation in vivo, we incubated cells prior to fixation for 30 minutes with 2 µM ZM447439 to reduce Aurora B kinase activity (Ditchfield et al., 2003). For all phosphorylation-specific Hec1 antibodies, there was a significant reduction in kinetochore fluorescence intensity after treatment with ZM447439 in PtK1, HeLa and U2OS cells (Fig. 3D; Fig. 4C,D; supplementary material Figs S1 and S2), indicating that Aurora B kinase activity is required for Hec1 phosphorylation on these residues in cells.

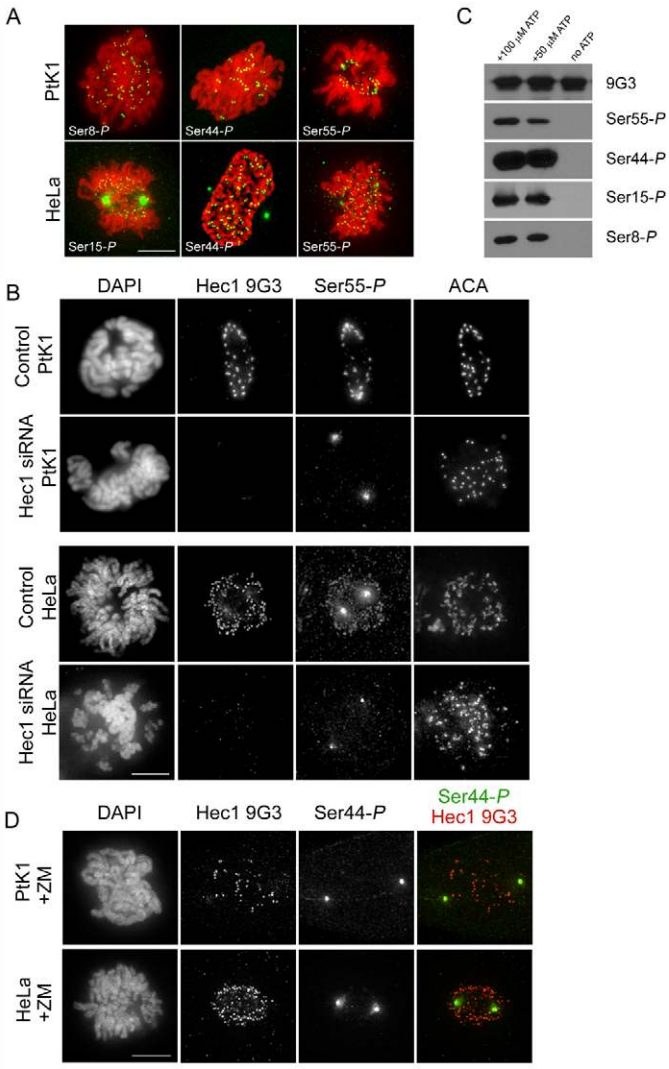

Fig. 3. Hec1 is phosphorylated at kinetochores on multiple N-terminal serine residues and phosphorylation is dependent on Aurora B kinase. (**A**) Immunofluorescence images of PtK1 and HeLa cells stained with Hec1 phosphorylation-specific antibodies. Antibodies raised against peptides containing phosphorylated Ser8, Ser44 and Ser55 recognized kinetochores consistently in PtK1 cells, and antibodies raised against peptides containing phosphorylated Ser15, Ser44 and Ser55 recognized kinetochores consistently in HeLa cells. (**B**) Immunofluorescence images of mock-depleted or Hec1-depleted PtK1 and HeLa cells probed for Ser55-*P*. Kinetochore localization of the anti-Ser55-*P* antibody and the Hec1 9G3 antibody is lost upon depletion of Hec1. (**C**) Immunoblots of recombinantly expressed and purified NDC80^{Bonsai} complexes probed with the non-phosphorylation-specific Hec1 9G3 antibody and the 4 phosphorylation-specific Hec1 antibodies. Purified NDC80^{Bonsai} complexes were incubated with activated Aurora B kinase in the presence or absence of ATP and subjected to SDS-PAGE prior to immunoblot analysis. (**D**) Immunofluorescence images of a PtK1 and HeLa cell treated with 2 µM ZM447439. Kinetochore localization of Ser44-*P* is significantly diminished in both cell types in response to treatment with the inhibitor.

Hec1 phosphorylation at kinetochores is high early in mitosis and decreases as chromosomes bi-orient

To determine the physiological relevance of Ser55, Ser44, Ser15 and Ser8 phosphorylation, we examined the timing of Hec1 phosphorylation at kinetochores during mitosis. The kinetochore

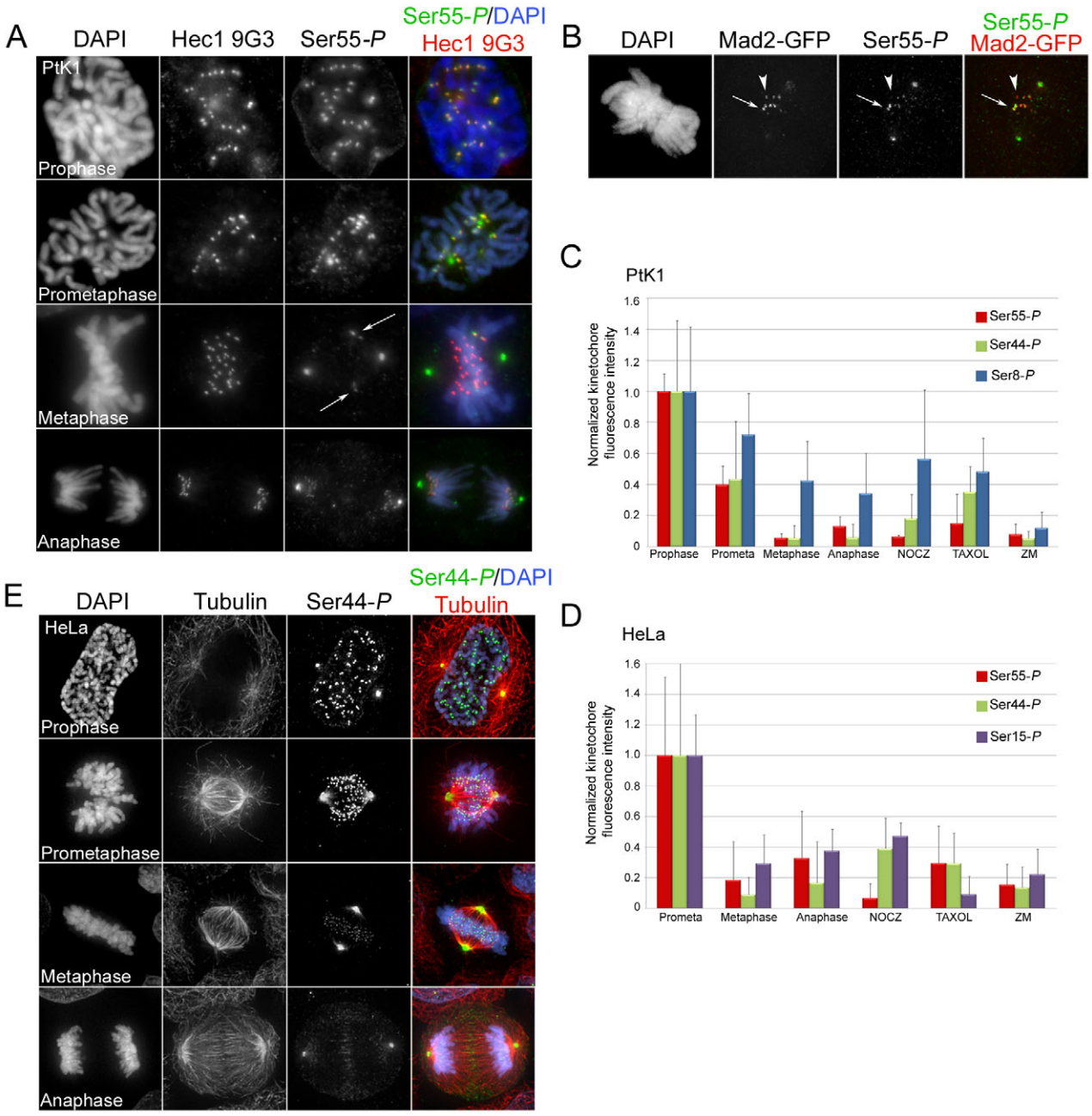

Fig. 4. Phosphorylation of Hec1 at kinetochores peaks in early mitosis and decreases as chromosomes bi-orient. (**A**) Localization of Ser55-*P* throughout mitosis in PtK1 cells. Cells were fixed and immunostained using a non-phosphorylation-specific Hec1 9G3 antibody and an antibody to Ser55-*P*. Arrows indicate sister kinetochore pairs whose inter-kinetochore axes are not parallel to the spindle axis. (**B**) Mad2–GFP localizes to kinetochores that are positive for Ser55-*P* staining in PtK1 cells. The arrow points to a kinetochore with high levels of both Mad2–GFP and Ser55-*P*, and the arrowhead points to a kinetochore with high levels of Mad2–GFP and low levels of Ser55-*P*. (**C**) Quantification of Ser55-*P*, Ser44-*P* and Ser8-*P* levels at kinetochores in PtK1 cells. For each phase of mitosis or drug condition, at least 100 kinetochores from 10 cells were quantified. In all cases, kinetochore fluorescence intensity was normalized to the fluorescence intensity of ACA. (**D**) Quantification of Ser55-*P*, Ser44-*P* and Ser15-*P* levels at kinetochores in HeLa cells. For each phase of mitosis or drug condition, at least 100 kinetochores from 10 cells were quantified. In all cases, kinetochore fluorescence intensity was normalized to the fluorescence intensity of ACA. For the quantification of kinetochores in nocodazole-treated cells in C and D, kinetochores were measured from drug-treated cells that had compact chromosome morphology, suggesting that they did not enter mitosis in the presence of the drug, but rather that the drug was added after some degree of chromosome alignment. (**E**) Localization of Ser44-*P* throughout mitosis in HeLa cells. Cells were fixed and immunostained using antibodies to Ser44-*P* and tubulin. Error bars indicate s.d.

localization of Ser55-*P* in PtK1 cells was maximally high in prophase, just before nuclear envelope breakdown. As cells progressed through mitosis, Ser55-*P* kinetochore levels decreased, reaching a minimal value at metaphase, when all chromosomes were aligned at the spindle equator and sister kinetochores had bi-oriented. A clear trend was evident in which kinetochores on chromosomes not properly aligned exhibited elevated levels of Ser55-*P* (Fig. 4A, arrows). To confirm that kinetochores with high levels of phosphorylated Hec1

were not properly attached to MTs, we analyzed cells expressing a GFP-tagged version of Mad2, a spindle assembly checkpoint protein that localizes to unattached kinetochores (Chen et al., 1996; Li and Benezra, 1996). As shown in Fig. 4B, kinetochores that exhibited high levels of Ser55-*P* also exhibited high levels of Mad2–GFP (arrow). Of note, kinetochores that retained high levels of phosphorylated Hec1 were almost always positive for Mad2–GFP. The reverse was not necessarily the case, as we were able to identify kinetochores that were positive for Mad2 but not for phosphorylated Hec1 (Fig. 4B, arrowhead). This suggests that Hec1 is dephosphorylated prior to complete depletion of Mad2 from kinetochores.

Quantification of kinetochore fluorescence intensities revealed a 93% decrease in Ser55-*P* at kinetochores from late prophase to metaphase (Fig. 4C). A similar temporal localization profile for Ser55-*P* was observed at kinetochores in HeLa cells, where kinetochore staining was high in early prometaphase and decreased by 80% as chromosomes congressed to the spindle equator (Fig. 4D; supplementary material Fig. S3). This staining pattern was also reproducible in U2OS cells (supplementary material Fig. S2). Similar localization patterns were observed for Ser44-*P* in PtK1, HeLa and U2OS cells, with levels reaching their maxima in early mitosis and decreasing as chromosomes aligned at the spindle equator (Fig. 4C–E; supplementary material Figs S2 and S4). Specifically, kinetochore fluorescence intensities of Ser44-*P* decreased from prophase to metaphase by 95% in PtK1 cells and from early prometaphase to metaphase by 86% in HeLa cells (Fig. 4C,D). Although both Ser8-*P* and Ser15-*P* (in PtK1 and HeLa cells, respectively) levels at kinetochores decreased during progression through mitosis, they did so modestly (a 50% reduction for Ser8-*P* and a 75% reduction for Ser15-*P*; Fig. 4C,D; supplementary material Figs S3 and S4). Together, these findings indicate that Hec1 is highly phosphorylated on its N-terminus in early mitosis when kinetochore–MT turnover is high, and that Hec1 is dephosphorylated in late mitosis when kinetochore–MT turnover is low (Zhai et al., 1995), suggesting that Hec1 phosphorylation influences kinetochore–MT stability during mitosis.

Phosphorylation on Hec1 Ser8, Ser15, Ser44 and Ser55 destabilizes kinetochore–MT attachments

We previously demonstrated that cells expressing a Hec1 mutant in which all nine putative Aurora B kinase target phosphorylation sites were mutated to mimic constitutive phosphorylation resulted in a defect in generating stable kinetochore–MT attachments (Guimaraes et al., 2008). To determine whether mimicking phosphorylation of the four identified in vivo targets (Ser8, Ser15, Ser44 and Ser55) is sufficient to perturb kinetochore–MT attachment, we depleted endogenous Hec1 from PtK1 cells and rescued with WT-Hec1–GFP or a Hec1 construct in which Ser8, Ser15, Ser44 and Ser55 were mutated to Asp ($SD^{8,15,44,55}$-Hec1–GFP) to mimic constitutive phosphorylation (supplementary material Fig. S5). PtK1 cells depleted of endogenous Hec1 and rescued with WT-Hec1–GFP generated stable kinetochore–MT attachments, as evidenced by the ability to align chromosomes at the spindle equator and to generate inter-kinetochore tension. By contrast, Hec1-depleted cells rescued with $SD^{8,15,44,55}$-Hec1–GFP failed to properly congress chromosomes to the spindle equator and exhibited a defect in generating inter-kinetochore tension when compared with control cells (supplementary material Fig. S5), indicating that stable kinetochore–MTs were not efficiently formed. We next generated additional Ser-to-Asp mutants, in which the number of amino acid mutations was reduced to three ($SD^{8,44,55}$-Hec1–GFP), two ($SD^{44,55}$-Hec1–GFP) or one (SD^{15}-Hec1–GFP). Cells rescued with $SD^{8,44,55}$-Hec1–GFP also experienced defects in both chromosome alignment and in forming stable kinetochore–MT attachments, as evidenced by a decrease in average inter-kinetochore distance (supplementary material Fig. S5). Cells rescued with either $SD^{44,55}$-Hec1–GFP or SD^{15}-Hec1–GFP, however, were able to align their chromosomes almost as well as cells rescued with WT-Hec1–GFP, and sister kinetochores were able to generate wild-type inter-kinetochore tension (supplementary material Fig. S5). These results suggest that multiple Hec1 tail-domain phosphorylation events are needed to impair kinetochore–MT stability.

A population of Aurora B kinase is enriched at the outer kinetochore in early mitosis

It has been proposed that phosphorylation of outer kinetochore targets by Aurora B is regulated by spatial positioning of the kinase, which is enriched at the centromere of mitotic chromosomes (Tanaka et al., 2002; Andrews et al., 2004; Liu et al., 2009). In such a model, under conditions of low centromere tension (prior to chromosome bi-orientation), outer kinetochore targets of Aurora B are proximal to centromeric Aurora B kinase, allowing for interaction and phosphorylation. Conversely, upon chromosome bi-orientation and generation of high centromere tension, outer kinetochore targets are physically separated from Aurora B kinase, preventing interaction and phosphorylation. To determine whether spatial positioning of Aurora B might regulate phosphorylation of Hec1, we immunolocalized active Aurora B kinase using an antibody against Thr232-*P*, which recognizes the phosphorylated active form of the kinase (Yasui et al., 2004), during progression through mitosis and compared its localization pattern with that of phosphorylated Hec1. In prophase PtK1 cells, active Aurora B kinase localized strongly to the outer kinetochore and also to the centromere (Fig. 5A). As cells progressed through mitosis, the outer kinetochore population of active Aurora B kinase decreased by ~75% (from prophase to metaphase) (Fig. 5A,C). Similar to phosphorylated Hec1, however, active Aurora B kinase levels remained high at outer kinetochores of chromosomes that had not yet congressed to the metaphase plate (Fig. 5A, late prometa). Similar results were observed for HeLa cells, in which active Aurora B kinase levels decreased from the outer kinetochore by ~50% from prometaphase to metaphase (Fig. 5B,D). Importantly, Thr232-*P* kinetochore staining was lost upon treatment with the Aurora B kinase inhibitor ZM447439 in both HeLa and PtK1 cells (Fig. 5E), whereas Aurora B–GFP remained localized to the centromere under this condition. Interestingly, we only detected Aurora B–GFP at the centromere and did not observe a significant population at the outer kinetochore; therefore, the possibility that the anti-Thr232-*P* antibody might recognize a phosphorylated substrate of Aurora B kinase at kinetochores cannot be formally excluded.

Hec1 is not maximally rephosphorylated in response to lack of attachment

It is possible that Hec1 is phosphorylated at kinetochores in response to lack of MT attachment or tension across centromeres because kinetochores that retain the highest levels of phosphorylated Hec1 correspond to chromosomes that have not yet bi-oriented. We tested this by treating cells with nocodazole, to depolymerize all spindle MTs, for 30 minutes prior to fixation and

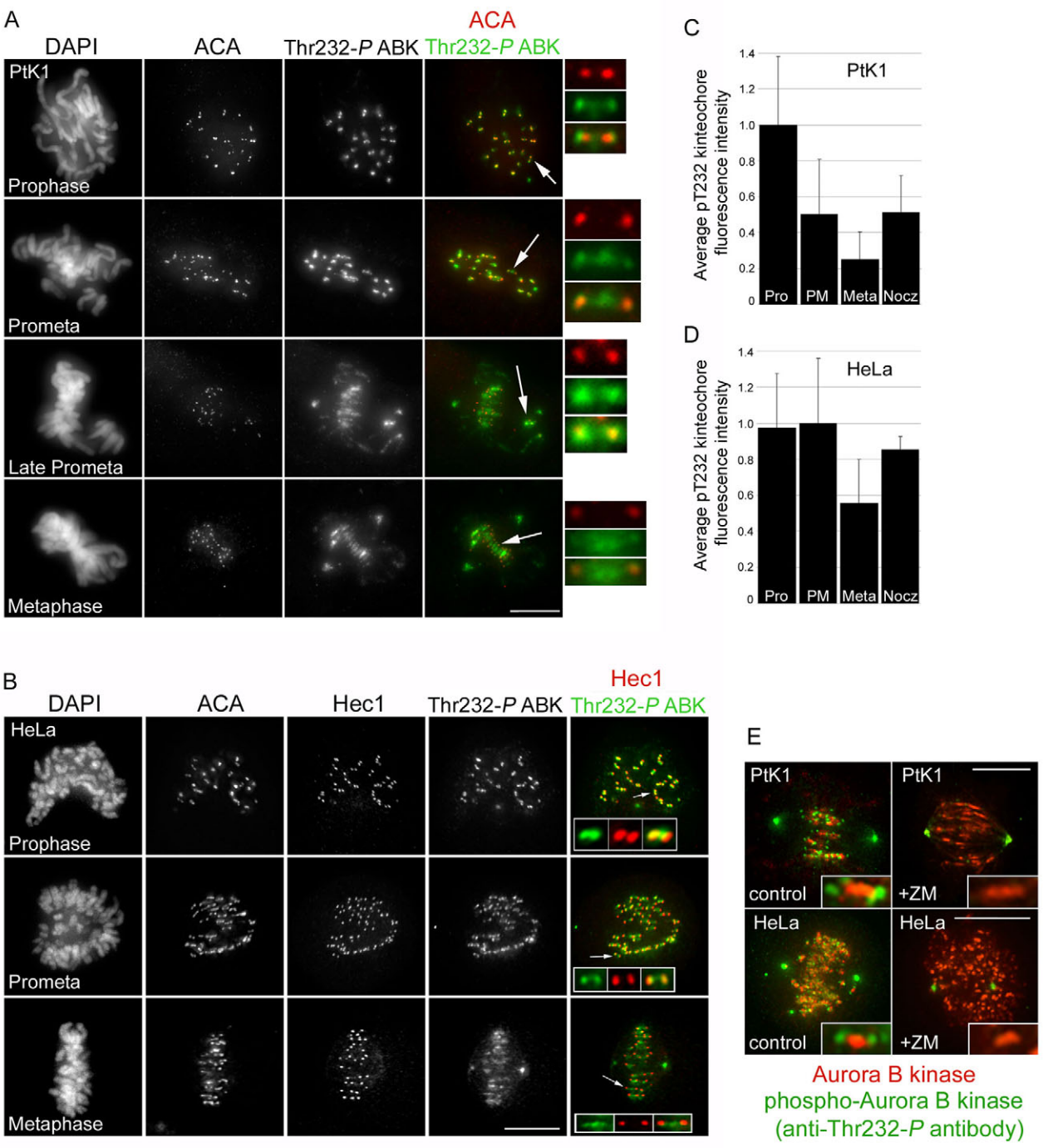

Fig. 5. Phosphorylated Aurora B kinase localizes to the centromere and kinetochore during mitosis. (**A**,**B**) Immunofluorescence images of PtK1 cells (A) and HeLa cells (B) in various stages of mitosis. Enlarged images and insets in A and B show kinetochore pairs (indicated by the arrows). (**C**,**D**) Quantification of phosphorylated Aurora B kinase at the outer kinetochore during mitosis. For each mitotic phase or condition, a minimum of 100 kinetochores were measured from a total of at least 10 cells. (**E**) Immunofluorescence images of PtK1 cells (top) and HeLa cells (bottom) expressing Aurora-B-kinase–GFP (shown as 'Aurora B kinase' and in red for clarity) treated with or without 2 µM ZM447439 prior to fixation and stained with anti-Thr232-*P* Aurora B kinase antibodies (green). Insets in E show individual representative kinetochore pairs for each condition. Scale bars: 10 µm. Error bars indicate s.d.

immunostaining with anti-Ser55-*P* antibodies. We reasoned that if Hec1 were phosphorylated in response to lack of MT attachment or tension, all kinetochores in mitotic nocodazole-treated cells would exhibit high levels of phosphorylated Hec1. Surprisingly, many mitotic cells treated with nocodazole did not contain kinetochores with high levels of phosphorylated Hec1, as evidenced by low anti-Ser55-*P* levels at kinetochores. In other cells, however, many or all kinetochores were positive for anti-Ser55-*P*. To understand the source of the variation, we examined PtK1 cell morphology as a function of mitotic progression in the presence of

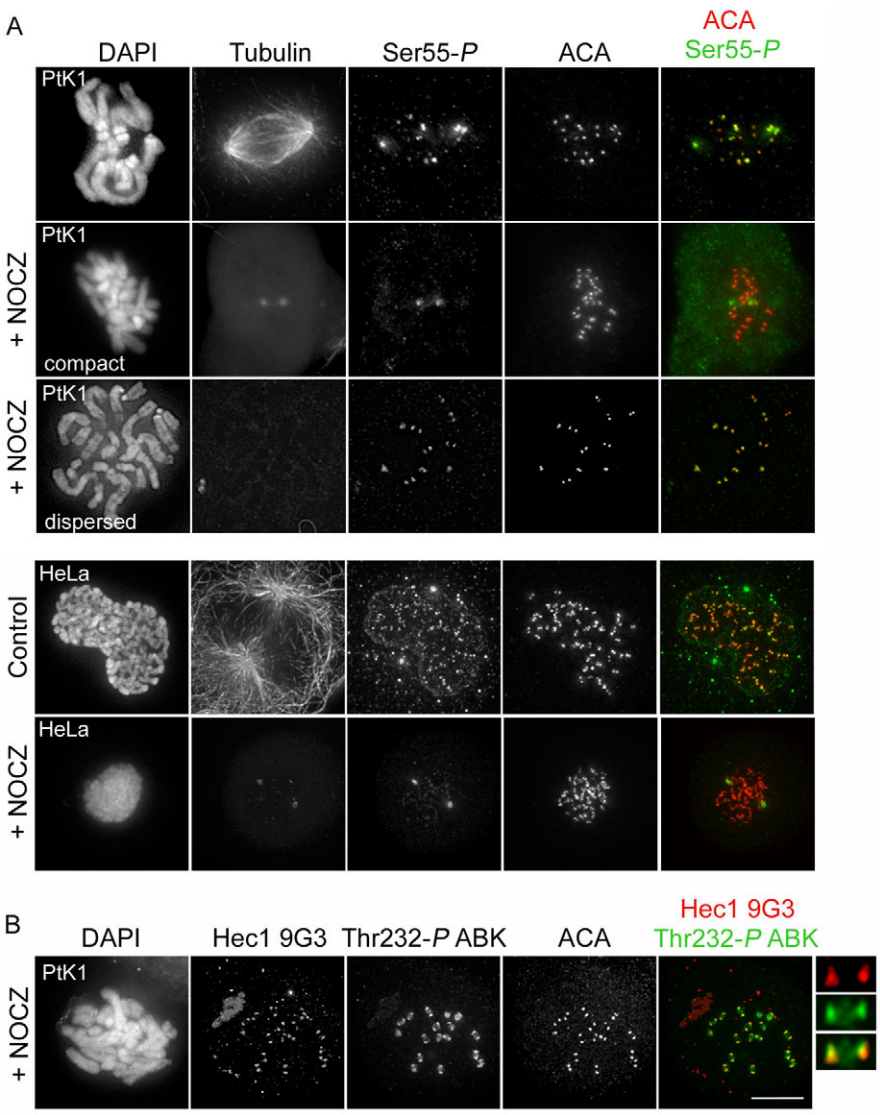

Fig. 6. Hec1 is not maximally rephosphorylated in response to lack of MT attachment.
(**A**) Immunofluorescence images of control PtK1 and HeLa cells and cells treated with nocodazole prior to fixation. In the top panel of images, an example is given of a PtK1 cell that has a 'compact' morphology, indicating that at least partial chromosome alignment occurred prior to incubation with nocodazole, and one that has a 'dispersed' morphology, indicating that the cell entered mitosis in the presence of nocodazole. (**B**) Immunofluorescence images of a PtK1 cell with compact chromosomes treated with nocodazole and stained with an anti-Thr232-*P* Aurora B kinase antibody. Enlarged images in B show a representative kinetochore pair from this experiment. Scale bar: 10 μm.

nocodazole and found that it was possible to approximate the status of chromosome alignment at the time of nocodazole treatment based on differences in chromosome morphology. Cells that entered mitosis in the presence of nocodazole exhibited a dispersed chromosome distribution, as expected in a scenario in which chromosomes have not generated attachments to MTs or aligned at the metaphase plate (Fig. 6A). Conversely, if metaphase cells were treated with nocodazole and MTs depolymerized after chromosomes had bi-oriented, their chromosome arrangement was more compact (Fig. 6A). We quantified anti-Ser55-*P* antibody reactivity and chromosome morphology in nocodazole and found that in all cells that exhibited low immunoreactivity at kinetochores (similar to those measured on kinetochores in control metaphase cells), the chromosomes were compact, indicating that these cells contained chromosomes that had already bi-oriented upon nocodazole treatment (Fig. 6A). Conversely, cells that contained many kinetochores positive for Ser55-*P* had a dispersed morphology, indicating that kinetochores in these cells contained high levels of phosphorylated Hec1 at the time of nocodazole addition (Fig. 6A). These results indicate that after Hec1 is dephosphorylated, it is not rephosphorylated to 'pre-attachment' levels in response to MT depolymerization. Similar results were obtained for Ser55-*P* in HeLa cells (Fig. 6A; Fig. 4D), although it was more difficult to differentiate between compact and dispersed chromosomes.

To determine whether the other phosphorylated residues exhibited the same behavior as Ser55-*P*, we carried out similar analyses using antibodies against Ser8-*P*, Ser15-*P* and Ser44-*P* (supplementary material Fig. S6). In both nocodazole-treated HeLa and PtK1 cells, Ser8-*P*, Ser15-*P* and Ser44-*P* exhibited localization patterns similar to those of Ser55-*P* (Fig. 4D; supplementary material Fig. S6), in which MT depolymerization by nocodazole treatment did not restore kinetochore fluorescence intensity levels of the phosphorylation-specific antibodies to those observed in late prophase or early prometaphase. We went on to test the effect of taxol, which stabilizes kinetochore–MT attachments but reduces inter-kinetochore tension, on Hec1 phosphorylation at kinetochores. Similar to loss of kinetochore–MT attachment, loss of kinetochore tension did not result in maximal rephosphorylation of Hec1 on any site in either PtK1 or HeLa cells (Fig. 4C,D; supplementary material Fig. S7). Why is Hec1 at kinetochores not maximally rephosphorylated in response to lack of MT attachment

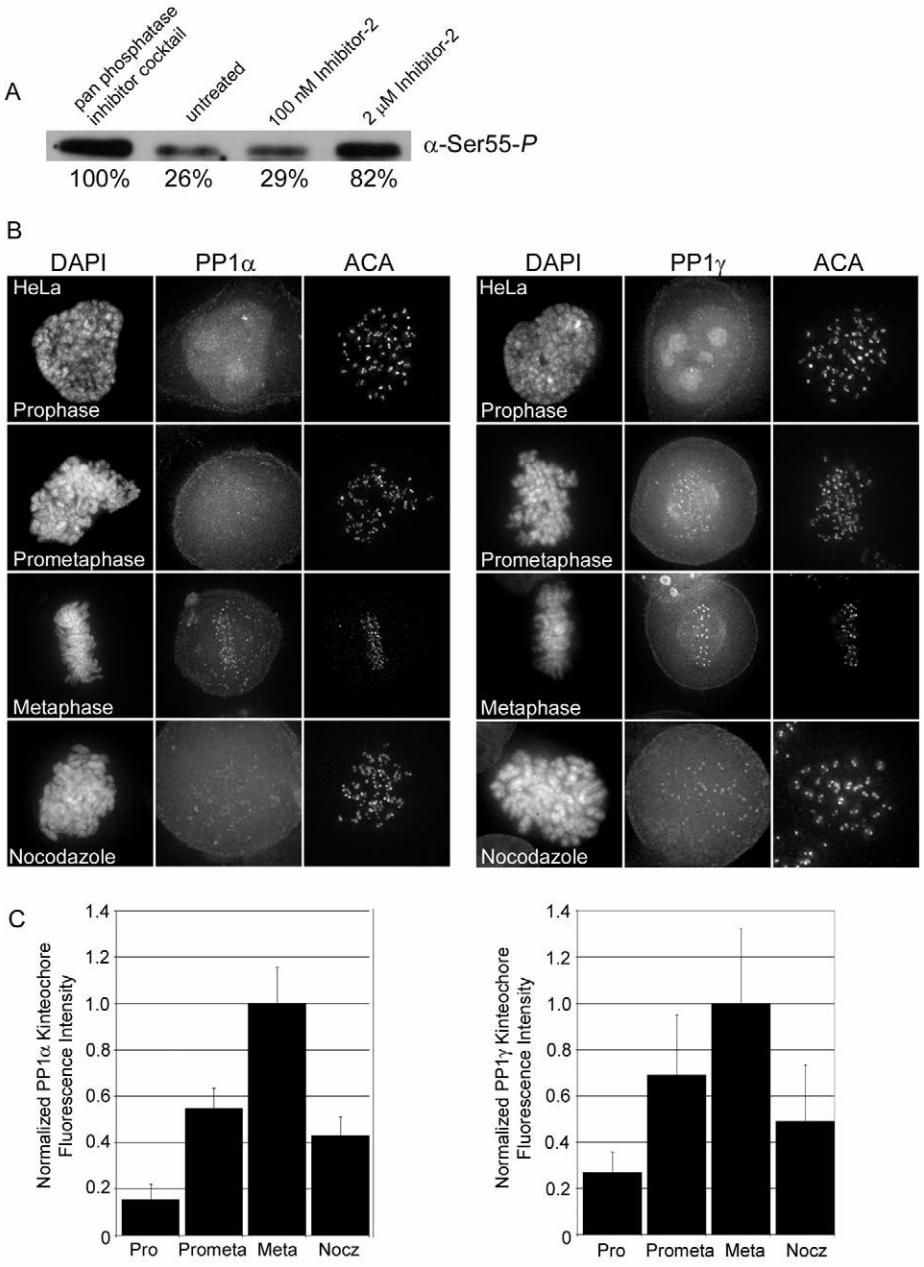

Fig. 7. Hec1 dephosphorylation by protein phosphatase 1. (**A**) Immunoblot of HeLa cell extracts treated with increasing concentrations of inhibitor 2 probed for Ser55-*P*. (**B**) Localization of GFP–PP1α and GFP–PP1γ in mitotic HeLa cells and in mitotic HeLa cells treated with nocodazole. (**C**) Quantification of kinetochore-localized GFP–PP1α and GFP–PP1γ. For each mitotic phase or condition, a minimum of 100 kinetochores were measured from a total of at least six cells. Error bars indicate s.d.

or tension? One possibility is that upon nocodazole treatment, active Aurora B kinase is depleted from the outer kinetochore, thus preventing phosphorylation of Hec1. To test this, we used the anti-Thr232-*P* antibody to quantify levels of active Aurora B kinase at the outer kinetochore in cells treated with nocodazole for 30 minutes (Fig. 6B). In PtK1 cells with compact chromosome morphology (cells that had aligned their chromosomes prior to nocodazole treatment), levels of active Aurora B kinase were decreased when compared with non-nocodazole-treated late-prophase cells, but only modestly (by ~50%; Fig. 5C). The same trend was observed in nocodazole-treated HeLa cells, where active Aurora B kinase levels at the outer kinetochore were only decreased by ~17% (Fig. 5D). This suggests that even in the presence of active Aurora B kinase at the outer kinetochore, Hec1 is not maximally rephosphorylated after chromosome bi-orientation and dephosphorylation have occurred.

Hec1 dephosphorylation by protein phosphatase 1

To investigate Hec1 dephosphorylation, we treated cell extracts with inhibitors of phosphatases known to localize to kinetochores during mitosis (Trinkle-Mulcahy and Lamond, 2006). When cell extracts were treated with increasing concentrations of protein phosphatase inhibitor 2, which potently inhibits the protein phosphatase 1 (PP1) family phosphatases (Cohen and Nimmo, 1978), and analyzed by SDS-PAGE and immunoblotting for Ser55-*P*, we measured a dose-dependent increase in immunoreactivity for Ser55-*P*, suggesting that PP1 is capable of dephosphorylating Hec1 (Fig. 7A). We next analyzed the localization patterns of PP1 phosphatases α and γ (two of the three closely related isoforms of PP1) at kinetochores during mitosis and compared them with the localization of Hec1 phosphorylation-specific antibodies. As shown in Fig. 7B and 7C, GFP–PP1α, and GFP–PP1γ exhibited weak kinetochore localization at the onset of mitosis and levels increased

as chromosomes gained alignment at the spindle equator (Trinkle-Mulcahy and Lamond, 2006; Liu et al., 2010). This is in contrast to the localization of Ser55-*P*, which was high at kinetochores in early mitosis and decreased significantly as chromosomes bi-oriented (Fig. 4). Our earlier results demonstrated that Hec1 is not maximally rephosphorylated upon loss of microtubule attachment or tension. To determine whether PP1 localization might be responsible for this lack of rephosphorylation, we tested whether PP1 remains at kinetochores after nocodazole treatment. In nocodazole-treated HeLa cells, we found that PP1 is present at kinetochores but that levels are significantly decreased from those observed at metaphase (Fig. 7B,C). Thus, although PP1 is able to dephosphorylate Hec1, it is probable that another factor is required for inhibition of rephosphorylation.

Discussion

Previous proteomics studies using isolated mitotic HeLa cell spindles or human embryonic stem cells have demonstrated that Hec1 is phosphorylated on Ser55 and Ser69 in vivo by undetermined kinases (Nousiainen et al., 2006; Malik et al., 2009; Brill et al., 2009; Olsen et al., 2010). We now include Ser44, Ser15 and Ser8 to the list of known in vivo N-terminal Hec1 phosphorylation sites (supplementary material Fig. S8), and have demonstrated here that phosphorylation on these sites is dependent on Aurora B kinase activity. Together with in vitro data demonstrating direct phosphorylation of Hec1 by Aurora B, these results suggest that Hec1 is a physiological target of Aurora B kinase during mitosis. Of note, the *C. elegans* Hec1 homolog (CeNDC80) contains only four predicted Ipl1 or Aurora B kinase phosphorylation sites (Ser51, Ser44, Ser18 and Thr8), and mutation of these sites eliminated phosphorylation of the protein by a purified Aurora kinase in vitro (Cheeseman et al., 2006). Sequence analysis indicates that the *C. elegans* residues Ser51, Ser44 and Ser18 correspond to the following human (and PtK1) residues: Ser55 (Ser60 for PtK1), Ser44 and Ser15, respectively (supplementary material Fig. S8). From our analysis of the Hec1 sequences, it is unclear whether *C. elegans* Thr8 corresponds to Ser5 or Ser8 in the human and PtK1 Hec1 sequences.

Interestingly, the anti-Ser8-*P* Hec1 antibody recognizes kinetochores in PtK1 cells but not in HeLa or U2OS cells. It is possible that Ser8 is not phosphorylated in human Hec1 or perhaps the anti-Ser8-*P* antibody cannot access this domain within the human Hec1 protein. Related to this point, antibodies generated specifically against Ser5-*P* did not recognize kinetochores in any cell type tested (data not shown). In addition, we generated an antibody to a peptide containing phosphorylated Ser62, which also did not recognize kinetochores in cells. We cannot rule out in vivo phosphorylation on these two residues, however, as the antibodies might have been unable to recognize their respective epitopes owing to inaccessibility. We did not generate phosphorylation-specific antibodies to Ser4, Thr49 and Ser69, thus the in vivo phosphorylation status of Ser4 and Thr49 remains unknown. We suspect that the identified target sites in this study represent physiologically relevant Aurora B kinase phosphorylation target sites for two reasons. First, as mentioned above, mutation of all four of these conserved target sites to alanine in CeNDC80 eliminated detectable in vitro phosphorylation by a purified Aurora kinase (Cheeseman et al., 2006). Second, PtK1 cells depleted of endogenous Hec1 and rescued with Hec1 mutants in which only three or four of the identified sites were mutated to Asp experienced defects in forming stable kinetochore–MT attachments (supplementary material Fig. S5). Given the published proteomic studies on Ser69 (Brill et al., 2009; Malik et al., 2009; Olsen et al., 2010), it will be interesting in the future to determine whether the temporal regulation of Ser69 phosphorylation is similar to that of the phosphorylated amino acids described here.

A key finding in this study is that Aurora-B-kinase-dependent Hec1 phosphorylation is high in early mitosis and significantly decreases as chromosomes bi-orient. This result provides a functional link between the observation that kinetochore–MT stability is low in early mitosis (Zhai et al., 1995) and the finding that Aurora B kinase is responsible for increasing kinetochore–MT turnover and inducing kinetochore–MT detachment (Cimini et al., 2006; Pinsky et al., 2006). We propose that in early mitosis, when attachment errors are most frequently made, phosphorylation of the Hec1 tail, which contributes to the linkage between kinetochores and MTs (Guimaraes et al., 2008; Miller et al., 2008), reduces the positive charge of the domain and thus decreases the affinity of kinetochores for negatively charged MTs. Conversely, dephosphorylation of the tail of Hec1 after chromosomes have bi-oriented ensures that kinetochore–MT attachments are stabilized in late mitosis so that forces can be generated for chromosome movements and to silence the mitotic spindle assembly checkpoint. Based on the findings that Hec1 N-terminal phosphorylation is significantly reduced after chromosome bi-orientation, it is probable that other mechanisms for inducing kinetochore–MT detachment and error correction are in place during late mitosis (Bakhoum et al., 2009). Recently, it has been demonstrated that both KNL1 and DSN1 (a member of the Mis12 complex) are phosphorylated in an Aurora-B-kinase-dependent manner in vivo, and phosphorylation of these proteins results in decreased affinity of the KMN complex for MTs in vitro (Welburn et al., 2010). Phosphorylated forms of both KNL1 and DSN1 at kinetochores decrease only modestly from prometaphase to metaphase (~33–55% reduction for KNL1-*P* and ~20% reduction for DSN1-*P*), thus it is possible that phosphorylation of these members of the KMN complex by Aurora B in late mitosis is sufficient to induce some level of kinetochore–MT turnover even in the absence of high levels of Hec1 phosphorylation. Another possibility is that the low levels of Hec1 phosphorylation observed during metaphase provide an adequate level of MT destabilization to allow for error correction in late mitosis and flexibility within the kinetochore–MT attachment site to allow for fluid plus-end MT dynamics and wild-type chromosome movements. Mutant analysis in this study supports the idea that some level of Hec1 phosphorylation is required for normal chromosome movements in metaphase because kinetochores in cells expressing nonphosphorylatable Hec1 (9A-Hec1–GFP) failed to undergo wild-type oscillations.

The results here suggest that Hec1-phosphorylation-dependent kinetochore–MT destabilization occurs specifically at kinetochores in early mitosis that are under low tension (i.e. on kinetochores of chromosomes that have not bi-oriented). It is somewhat surprising that in the presence of nocodazole, kinetochore-associated Hec1 is not rephosphorylated to pre-attachment levels. We can rule out the possibility that the drug modulates the binding site of the Hec1 N-terminus to prevent antibody accessibility because cells that enter mitosis in the presence of nocodazole retain high levels of phosphorylated Hec1. Rather, our data indicate that once Hec1 has been dephosphorylated, rephosphorylation to the level observed in late prophase and early prometaphase cells is inhibited. In the presence of nocodazole, active Aurora B kinase levels (detected using the anti-Thr232-*P* antibody) are only modestly reduced at

the outer kinetochore (Fig. 5), suggesting that prevention of rephosphorylation is not regulated solely at the level of kinase localization. It is probable that an additional factor binds to kinetochores upon dephosphorylation and prevents rephosphorylation to pre-attachment levels, even in the presence of nocodazole. The phosphatase PP1, which is able to dephosphorylate Hec1, might participate in this process by joining kinetochores after attachment to MTs and dephosphorylating kinetochore targets until mitotic exit. A recent report demonstrating that PP1 is targeted to kinetochores in late mitosis by the KMN component KNL1 lends support to this notion (Liu et al., 2010). This group further reported that phosphorylation of KNL1 on sites Ser24 and Ser60 by Aurora B kinase negatively regulates PP1 binding to KNL1 as a phosphomimetic version of KNL1 bound to PP1 in vitro with much less affinity than did wild-type KNL1 (Liu et al., 2010). A later study demonstrated that KNL1 Ser24 and Ser60 are phosphorylated at kinetochores in vivo in an Aurora-B-kinase-dependent manner and, as mentioned above, using phosphorylation-specific antibodies, these authors measured a 30–50% decrease in phosphorylated KNL1 on kinetochores from prometaphase to metaphase (Welburn et al., 2010). Presumably, this reduction of phosphorylation on KNL1 at kinetochores is sufficient to increase the affinity of KNL1 for PP1 so that kinetochore targets can be dephosphorylated. In this study, we report a 50–75% decrease in active Aurora B kinase at the outer kinetochore (in HeLa and PtK1 cells, respectively) from prometaphase to metaphase. It is possible that the decrease in active Aurora B kinase at the outer kinetochore is responsible for the drop in KNL1 phosphorylation and the subsequent recruitment of PP1 to the kinetochore and dephosphorylation of appropriate targets. In the specific case of Hec1, however, it is probable that an additional factor, yet to be identified, prevents high levels of Hec1 rephosphorylation after dephosphorylation because, after incubation in nocodazole, both phosphorylated Hec1 and PP1 levels are low at kinetochores.

How does Aurora B regulate kinetochore–MT attachment stability through Hec1 phosphorylation? One model proposes that outer kinetochore substrates of Aurora B are regulated by a change in spatial positioning of the kinase during progression through mitosis. Aurora B localizes prominently to the centromere region of mitotic chromosomes and it has been suggested that a gradient of Aurora B kinase originating from the centromere can only 'reach' outer kinetochore substrates such as Hec1 when sister kinetochores are under low tension (Tanaka et al., 2002; Andrews et al., 2004; Pinsky et al., 2006). In support of this, a recent study found that phosphorylation of an engineered Aurora B substrate at the kinetochore was dependent on its distance from the centromere and, furthermore, that experimentally positioning Aurora B closer to the outer kinetochore prevented stabilization of bi-oriented kinetochore–MT attachments (Liu et al., 2009). In regard to Aurora B phosphorylation of Hec1 specifically, our results are not fully consistent with a spatial positioning model for two reasons. First, antibodies to active Aurora B kinase localize to the outer kinetochore in both HeLa and PtK1 cells throughout mitosis, with levels decreasing only modestly from early prometaphase to metaphase. Conversely, Hec1 phosphorylation at kinetochores decreases from early prometaphase to metaphase by 95% for certain target sites. Thus, significant levels of the kinase remain at the outer kinetochore under conditions in which Hec1 is largely dephosphorylated. Second, Hec1 phosphorylation levels at kinetochores do not return to those measured in late prophase or early prometaphase in response to reduced inter-kinetochore tension brought on by incubation with high concentrations of nocodazole. Under this experimental condition, active Aurora B kinase remains at the outer kinetochore, indicating that although the kinase is spatially positioned to rephosphorylate Hec1, it does not. Because it is probable that other outer kinetochore targets are regulated by spatial positioning of the kinase (Liu et al., 2009; Liu et al., 2010; Welburn et al., 2010), the mechanism controlling Aurora-B-dependent phosphorylation cycles might differ between kinetochore targets.

Materials and Methods

Cell culture and drug treatments

PtK1 cells were cultured in Ham's F-12 medium supplemented with 10% fetal bovine serum (FBS), antibiotics and antimycotics and maintained at 37°C at 5% CO_2. HeLa cells were cultured in Dulbecco's Modified Eagle's Medium (DMEM) supplemented with 10% FBS, antibiotics and antimycotics and maintained at 37°C at 5% CO_2. For PP1 experiments, HeLa cells stably expressing either GFP–PP1α or GFP–PP1γ (generous gifts from Laura Trinkle-Mulcahy, University of Ottawa, Ottawa, Canada), were grown under the same conditions as HeLa cells, except that cells were supplemented with 200 μg/ml G418. Cells were grown on sterile, acid-washed coverslips in 35 mm Petri dishes or in 6-well plates. For live-cell imaging, coverslips were grown in 35 mm glass-bottom culture dishes (MatTek Corp., Ashland, MA) and imaged in Leibovitz's L-15 media (Invitrogen) supplemented with 10% FBS, 7 mM HEPES, pH 7.0 and 4.5 g/l glucose. For Aurora B kinase inhibition experiments, cells were treated with 2 μM ZM447439 (Tocris Cookson, Inc., Ellisville, MO) for 30 minutes prior to fixation and processing for immunofluorescence. For monastrol and monastrol washout experiments, cells were treated with 150 μM monastrol for 2 hours and either directly processed for immunofluorescence or washed 4 times with fresh medium containing 10 μM MG132 (or medium containing 10 μM ZM447439 + 10 μM MG132) and incubated for 20 or 60 minutes at 37°C prior to fixation and processing for immunostaining. For MT depolymerization experiments, cells were treated with 20 μM nocodazole (Sigma) for 30 minutes prior to fixation for immunofluorescence.

Transient transfections: siRNA and DNA

For Hec1 silence and rescue experiments, either lipid-based transfection or electroporation techniques were used. For lipid-based transfection, per coverslip, 7 μl oligofectamine was incubated at room temperature with 143 μl of OptiMem (Invitrogen) for 5 minutes. Subsequently, 8 μl of 20 μM PtK1-specific Hec1 siRNA (Guimaraes et al., 2008) or human-specific Hec1 siRNA targeted to the 5′ UTR (CCCUGGGUCGUGUCAGGAA), 2 μl of plasmid DNA (1 mg/ml) and 142 μl of OptiMem were added to the tube and allowed to incubate for 20–30 minutes at room temperature. Following incubation, the solution was added to 2 ml of Optimem + 10% FBS and added to a coverslip in a 6-well dish. Cells were supplemented with 1 ml of OptiMem + 10% FBS 24 hours post-transfection and assayed at 48 hours post-transfection. For electroporation-based transfection, PtK1 cells were transfected using the Nucleofector (Lonza, Germany). Cells were transfected according to the manufacturer's instructions using program T-021 and the same concentrations of siRNA and DNA mentioned above. The following DNA plasmids were used: Mad2–GFP (a gift from Guowei Fang, Stanford University, Palo Alto, CA), GFP–PP1γ and GFP–PP1α (gifts from Laura Trinkle-Mulcahy), GFP–Aurora-B (a gift from Yu-Li Wang, UMASS Medical School, Worcester, MA), WT-Hec1–GFP (Guimaraes et al., 2008) and 9A-Hec1–GFP (Guimaraes et al., 2008). The phosphomimetic Hec1 constructs $SD^{8,15,44,55}$-Hec1–GFP, $SD^{8,44,55}$-Hec1–GFP, $SD^{44,55}$-Hec1–GFP and SD^{15}-Hec1–GFP were generated using a QuikChange Site-Directed Mutagenesis Kit (Stratagene).

Immunofluorescence

Cells were rinsed rapidly in 37°C PHEM buffer (60 mM PIPES, 25 mM HEPES, 10 mM EGTA, 4 mM $MgSO_4$, pH 6.9) followed by a 5 second fixation at 37°C in 4% paraformaldehyde freshly prepared from a 16% stock solution (Ted Pella Inc., Redding, CA). Cells were then lysed at 37°C for 5 minutes in freshly prepared lysis buffer (PHEM buffer + 1.0% Triton X-100) containing 100 nM microcystin (Sigma-Aldrich), followed by fixation for 20 minutes at room temperature in 4% paraformaldehyde in PHEM buffer pre-warmed to 37°C. At room temperature, cells were rinsed 3×5 minutes in PHEM-T (PHEM buffer + 0.1% Triton-X-100) and blocked in 10% boiled donkey serum (BDS) in PHEM for 1 hour at room temperature. Primary antibodies diluted in 5% BDS were added to coverslips and allowed to incubate for 12 hours at 4°C. The following commercially available primary antibody dilutions were used: mouse anti-Hec1 9G3 at 1:3000 (Novus Biologicals, Littleton, CO), human anti-centromere antibody at 1:300 (ACA; Antibodies, Inc., Davis, CA), DM1α mouse anti-tubulin at 1:200 (Sigma); rat anti-tubulin at 1:200 (Sigma); and rabbit anti-phosphorylated Aurora-B (Thr232-*P*) at 1:1000 (Rockland Immunochemicals, Gilbertsville, PA). Following primary antibody incubation, cells were rinsed 3×5 minutes in PHEM-T and then incubated for 45 minutes at room temperature with secondary antibodies conjugated to either Cy5, Alexa Fluor 488 or

Rhodamine RedX (Jackson ImmunoResearch Laboratories) and diluted in 5% BDS to 1:300. Cells were rinsed 3×5 minutes in PHEM-T, incubated in a solution of 2 ng/ml 4′,6-diamidino-2-phenylindole (DAPI) diluted in PHEM, rinsed again (3×5 minutes), quick-rinsed in PHEM then mounted onto microscope slides in an anti-fade solution containing 90% glycerol and 0.5% *N*-propyl gallate. Coverslips were sealed with nail polish to affix them to the slides.

Hec1 phosphorylation-specific antibody production

Affinity-purified antibodies against phosphorylated Ser55 were generated at Open Biosystems (Huntsville, AL). Rabbits were immunized with a phosphorylated peptide corresponding to amino acids 47–60 in the N-terminus of Hec1. Affinity-purified antibodies against phosphorylated Ser8, Ser15 and Ser44 were generated at 21st Century Biochemicals (Marlboro, MA). Rabbits were immunized with phosphorylated peptides corresponding to the following amino acids in the N-terminus of human Hec1: 1–15 (Ser8-*P*), 8–23 (Ser15-*P*) and 38–51 (Ser44-*P*).

Image acquisition and analysis

Fixed-cell image acquisition was carried out on a DeltaVision PersonalDV Imaging System (Applied Precision, Issquah, WA) equipped with a Photometrics CoolSnap HQ2 camera (Roper Scientific, Sarasota, FL) and a 60×/1.42NA Planapochromat DIC oil immersion lens (Olympus). For immunofluorescence experiments, *z*-stacks at 0.2 μm intervals were acquired through each cell. Kinetochore fluorescence intensity measurements were carried out using Metamorph software (MDS Analytical Technologies), in which the intensity of a test protein was calculated by determining the ratio of its total integrated intensity to the intensity of ACA (anti-centromere antibody) staining at the same kinetochore. Microtubule end-on attachment was scored using SoftWorx software (Applied Precision) by analyzing *z*-stacks of deconvolved images.

For live-cell imaging of kinetochore oscillations, stage temperature was maintained at 37°C with an environmental chamber (Precision Control, Seattle, WA). Fluorescence images of GFP–Hec1-expressing cells were acquired using a 60×/1.42NA DIC Planapochromat oil immersion lens (Olympus) every 3 seconds for 10 minutes. At each time-point, three images were collected in a *z*-through series using a 0.5 μm step size. Cells were chosen for analysis based on both positive GFP-fusion protein expression and Cy5-labeled siRNA transfection. For all measurements, measured kinetochores were located within the middle of the spindle. Cells that did not exhibit significant drift were chosen for analysis; therefore, movements were not tracked in relation to a fixed point. Kinetochore movements were tracked on maximum projection movies using the 'track points' function in Metamorph software. Velocity and percent pause were determined using Metamorph software. A 'pause' event was recorded when a kinetochore did not move for two sequential time frames (6 seconds). The percentage of time spent in pause was determined by dividing the sum of time spent in pause by the total time of the time-lapse sequence. The deviation from average position, developed by Stumpff et al. (Stumpff et al., 2008), was determined using SigmaPlot software (Systat Software, Chicago, IL). To calculate the deviation from average position, time and distance data were exported into SigmaPlot, where a scatter plot (time on the *x*-axis, distance on the *y*-axis) was created. A linear regression line was then fit to the plot and the position on the regression line was subtracted from the corresponding original kinetochore position. This produced a distance value for each time-point, which represented the distance away from the average position of that kinetochore. These numbers were averaged to produce the final deviation from average position value.

Preparation of cell lysates and immunoblotting

For control and drug treatments, cells were grown in 150 cm^2 flasks to 80% confluency. Cells were harvested from the flasks with trypsin, pelleted in a tabletop centrifuge and raised in cold 1× PBS (140 mM NaCl, 2.5 mM KCl, 1.6 mM KH_2PO_4, 15 mM Na_2HPO_4, pH 7.0) + 2 mM DTT + protease inhibitor cocktail (Sigma). Cells were sonicated on ice (Ultra Sonic Device) and lysates were clarified by centrifugation. Samples were run on 12% SDS-polyacrylamide gels and transferred to PVDF membrane (Millipore). For Hec1 staining, blots were probed with mouse anti-Hec1 (Novus Biologicals) at 1:1000. For tubulin staining, blots were probed with mouse anti-α-tubulin (Sigma) at 1:2000. Antibodies were detected using a horseradish peroxidase-conjugated-anti-mouse secondary antibody at 1:10,000 (Jackson ImmunoResearch Laboratories) and enhanced chemiluminescence (Thermo Scientific).

Protein purification and in vitro kinase assays

$NDC80^{Bonsai}$ was expressed and purified as described in Ciferri et al. (Ciferri et al., 2008). Aurora B kinase and $INCENP^{790–856}$ proteins were expressed and purified as described in Sessa et al. (Sessa et al., 2005). For kinase assays, Aurora B was pre-activated by incubation of 0.5 μg Aurora B + 0.5 μg $INCENP^{790–856}$ with 50 μM ATP, 27.5 mM $MgCl_2$ in kinase buffer (6.7 mM Tris-HCl pH 7.5, 0.013 mM EGTA, 2 mM DTT) for 10 minutes at 30°C. Purified $NDC80^{Bonsai}$ (1 μg) was added to the pre-activated kinase and allowed to incubate for 20 minutes at 30°C. Reactions were terminated by the addition of 5× SDS-PAGE sample buffer and subjected to analysis by SDS-PAGE. Samples were transferred onto PVDF membranes and processed for immunoblotting using phosphorylation-specific Hec1 antibodies or non-phosphorylation specific Hec1 antibodies (9G3) as described above.

The authors thank Geoff Guimaraes for generation of the phosphomimetic constructs, Jeanne Mick for protein purification, Betsy Buechler and Martijn Vromans for technical assistance and data quantification, and Jason Stumpff for helpful conversations regarding kinetochore oscillations. The authors also thank Laura Trinkle-Mulcahy, Kevin Vaughan, Andrea Musacchio, Guowei Fang, Yu-Li Wang and Ted Salmon for providing reagents. This work was supported by National Institutes of Health grants K01CA125051 and R01534521 to J.G.D. and by a Basil O'Conner Starter Scholar Research Award to J.G.D. J.G.D. is also supported by the Pew Scholars Program in the Biomedical Sciences. S.M.A.L. is supported by the Netherlands Organization for Scientific Research (Vidi 917.66.332) and the Dutch Cancer Society (KWF-UU 2009-4311). Deposited in PMC for release after 12 months.

Supplementary material available online at
http://jcs.biologists.org/cgi/content/full/124/4/622/DC1

References

Andrews, P. D., Ovechkina, Y., Morrice, N., Wagenbach, M., Duncan, K., Wordeman, L. and Swedlow, J. R. (2004). Aurora B regulates MCAK at the mitotic centromere. *Dev. Cell* **6**, 253-268.

Akiyoshi, B., Nelson, C.R., Ranish, J.A. and Biggins, S. (2009) Analysis of Ipl1-mediated phosphorylation of the Ndc80 kinetochore protein in *Saccharomyces cerevisiae*. *Genetics* **183**,1591-1595.

Bakhoum, S. F., Thompson, S. L., Manning, A. L. and Compton, D. A. (2009). Genome stability is ensured by temporal control of kinetochore-microtubule dynamics. *Nat. Cell Biol.* **11**, 27-35.

Biggins, S. and Murray, A. W. (2001). The budding yeast protein kinase Ipl1/Aurora allows the absence of tension to activate the spindle checkpoint. *Genes Dev.* **15**, 3118-3129.

Brill, L. M., Xiong, W., Lee, K. B., Ficarro, S. B., Crain, A., Xu, Y., Terskikh, A., Snyder, E. Y. and Ding, S. (2009). Phosphoproteomic analysis of human embryonic stem cells. *Cell Stem Cell* **5**, 204-213.

Cheeseman, I. M., Anderson, S., Jwa, M., Green, E. M., Kang, J., Yates, J. R., III, Chan, C. S., Drubin, D. G. and Barnes, G. (2002). Phospho-regulation of kinetochore-microtubule attachments by the Aurora kinase Ipl1p. *Cell* **111**, 163-172.

Cheeseman, I. M., Chappie, J. S., Wilson-Kubalek, E. M. and Desai, A. (2006). The conMcserved KMN network constitutes the core microtubule-binding site of the kinetochore. *Cell* **127**, 983-997.

Chen, R. H., Waters, J. C., Salmon, E. D. and Murray, A. W. (1996). Association of spindle assembly checkpoint component XMAD2 with unattached kinetochores. *Science* **274**, 242-246.

Chen, Y., Riley, D. J., Chen, P. L. and Lee, W. H. (1997). HEC, a novel nuclear protein rich in leucine heptad repeats specifically involved in mitosis. *Mol. Cell. Biol.* **17**, 6049-6056.

Ciferri, C., Pasqualato, S., Screpanti, E., Varetti, G., Santaguida, S., Dos Reis, G., Maiolica, A., Polka, J., DeLuca, J. G., De Wulf, P. et al. (2008). Implications for kinetochore-microtubule attachment from the structure of an engineered Ndc80 complex. *Cell* **133**, 427-439.

Cimini, D. (2008). Merotelic kinetochore orientation, aneuploidy, and cancer. *Biochim. Biophys. Acta* **1786**, 32-40.

Cimini, D., Cameron, L. A. and Salmon, E. D. (2004). Anaphase spindle mechanics prevent mis-segregation of merotelically oriented chromosomes. *Curr. Biol.* **14**, 2149-2155.

Cimini, D., Wan, X., Hirel, C. B. and Salmon, E. D. (2006). Aurora kinase promotes turnover of kinetochore microtubules to reduce chromosome segregation errors. *Curr. Biol.* **16**, 1711-1718.

Cohen, P. and Nimmo, G. A. (1978). The purification and characterization of protein phosphatase inhibitor-1 from rabbit skeletal muscle. *Biochem. Soc. Trans.* **6**, 17-20.

DeLuca, J. G., Moree, B., Hickey, J. M., Kilmartin, J. V. and Salmon, E. D. (2002). hNuf2 inhibition blocks stable kinetochore-microtubule attachment and induces mitotic cell death in HeLa cells. *J. Cell Biol.* **159**, 549-555.

DeLuca, J. G., Gall, W. E., Ciferri, C., Cimini, D., Musacchio, A. and Salmon, E. D. (2006). Kinetochore microtubule dynamics and attachment stability are regulated by Hec1. *Cell* **127**, 969-982.

Ditchfield, C., Johnson, V. L., Tighe, A., Ellston, R., Haworth, C., Johnson, T., Mortlock, A., Keen, N. and Taylor, S. S. (2003). Aurora B couples chromosome alignment with anaphase by targeting BubR1, Mad2, and Cenp-E to kinetochores. *J. Cell Biol.* **161**, 267-280.

Guimaraes, G., Dong, Y., McEwen, B. F. and DeLuca, J. G. (2008). Kinetochore-microtubule attachment relies on the disordered N-terminal tail domain of Hec1. *Curr. Biol.* **18**, 1778-1784.

Hauf, S., Cole, R. W., LaTerra, S., Zimmer, C., Schnapp, G., Walter, R., Heckel, A., van Meel, J., Rieder, C. L. and Peters, J. M. (2003). The small molecule Hesperadin reveals a role for Aurora B in correcting kinetochore-microtubule attachment and in maintaining the spindle assembly checkpoint. *J. Cell Biol.* **161**, 281-294.

Kapoor, T. M., Mayer, T. U., Coughlin, M. L. and Mitchison, T. J. (2000). Probing spindle assembly mechanisms with monastrol, a small molecule inhibitor of the mitotic kinesin, Eg5. *J. Cell Biol*. **150**, 975-988.

Knowlton, A. L., Lan, W. and Stukenberg, P. T. (2006). Aurora B is enriched at merotelic attachment sites, where it regulates MCAK. *Curr. Biol*. **16**, 1705-1710.

Lampson, M. A. and Kapoor, T. M. (2005). The human mitotic checkpoint protein BubR1 regulates chromosome-spindle attachments. *Nat. Cell Biol*. **7**, 93-98.

Li, Y. and Benezra, R. (1996). Identification of a human mitotic checkpoint gene: hsMAD2. *Science* **274**, 246-248.

Liu, D., Vader, G., Vromans, M. J., Lampson, M. A. and Lens, S. M. (2009). Sensing chromosome bi-orientation by spatial separation of aurora B kinase from kinetochore substrates. *Science* **323**, 1350-1353.

Liu, D., Vleugel, M., Backer, C. B., Hori, T., Fukagawa, T., Cheeseman, I. M. and Lampson, M. A. (2010). Regulated targeting of protein phosphatase 1 to the outer kinetochore by KNL1 opposes Aurora B kinase. *J. Cell Biol*. **188**, 809-820.

Malik, R., Lenobel, R., Santamaria, A., Ries, A., Nigg, E. A. and Körner, R. (2009). Quantitative analysis of the human spindle phosphoproteome at distinct mitotic stages. *J. Proteome Res*. **8**, 4553-4563.

Martin-Lluesma, S., Stucke, V. M. and Nigg, E. A. (2002). Role of Hec1 in spindle checkpoint signaling and kinetochore recruitment of Mad1/Mad2. *Science* **297**, 2267-2270.

Mayer, T. U., Kapoor, T. M., Haggarty, S. J., King, R. W., Schreiber, S. L. and Mitchison, T. J. (1999). Small molecule inhibitor of mitotic spindle bipolarity identified in a phenotype-based screen. *Science* **286**, 971-974.

McCleland, M. L., Kallio, M. J., Barrett-Wilt, G. A., Kestner, C. A., Shabanowitz, J., Hunt, D. F., Gorbsky, G. J. and Stukenberg, P. T. (2004). The vertebrate Ndc80 complex contains Spc24 and Spc25 homologs, which are required to establish and maintain kinetochore-microtubule attachment. *Curr. Biol*. **14**, 131-137.

Miller, S. A., Johnson, M. L. and Stukenberg, P. T. (2008). Kinetochore attachments require an interaction between unstructured tails on microtubules and Ndc80(Hec1). *Curr. Biol*. **18**, 1785-1791.

Nousiainen, M., Sillje, H. H., Sauer, G., Nigg, E. A. and Korner, R. (2006). Phosphoproteome analysis of the human mitotic spindle. *Proc. Natl. Acad. Sci. USA* **103**, 5391-5396.

Olsen, J. V., Vermeulen, M., Santamaria, A., Kumar, C., Miller, M. L., Jensen, L. J., Gnad, F., Cox, J., Jensen, T. S., Nigg, E. A. et al. (2010). Quantitative phosphoproteomics reveals widespread full phosphorylation site occupancy during mitosis. *Sci. Signal*. **3**, ra3.

Pinsky, B. A., Kung, C., Shokat, K. M. and Biggins, S. (2006). The Ipl1-Aurora protein kinase activates the spindle checkpoint by creating unattached kinetochores. *Nat. Cell Biol*. **8**, 78-83.

Sessa, F., Mapelli, M., Ciferri, C., Tarricone, C., Areces, L. B., Schneider, T. R., Stukenberg, P. T. and Musacchio, A. (2005). Mechanism of Aurora B activation by INCENP and inhibition by hesperadin. *Mol. Cell* **18**, 379-391.

Stumpff, J., von Dassow, G., Wagenbach, M., Asbury, C. and Wordeman, L. (2008). The kinesin-8 motor Kif18A suppresses kinetochore movements to control mitotic chromosome alignment. *Dev. Cell* **14**, 252-262.

Tanaka, T. U., Rachidi, N., Janke, C., Pereira, G., Galova, M., Schiebel, E., Stark, M. J. and Nasmyth, K. (2002). Evidence that the Ipl1-Sli15 (Aurora kinase-INCENP) complex promotes chromosome bi-orientation by altering kinetochore-spindle pole connections. *Cell* **108**, 317-329.

Tien, A. C., Lin, M. H., Su, L. J., Hong, Y. R., Cheng, T. S., Lee, Y. C., Lin, W. J., Still, I. H. and Huang, C. Y. (2004). Identification of the substrates and interaction proteins of aurora kinases from a protein-protein interaction model. *Mol. Cell. Proteomics* **3**, 93-104.

Trinkle-Mulcahy, L. and Lamond, A. I. (2006). Mitotic phosphatases: no longer silent partners. *Curr. Opin. Cell Biol*. **18**, 623-631.

Vader, G., Maia, A. F. and Lens, S. M. (2008). The chromosomal passenger complex and the spindle assembly checkpoint: kinetochore-microtubule error correction and beyond. *Cell Div*. **3**, 10-19.

Wei, R. R., Al-Bassam, J., Harrison, S. C. (2007). The Ndc80/HEC1 complex is a contact point for kinetochore-microtubule attachment. *Nat. Struct. Mol. Biol*. **14**, 54-59.

Welburn, J. P., Vleugel, M., Liu, D., Yates, J. R., III, Lampson, M. A., Fukagawa, T. and Cheeseman, I. M. (2010). Aurora B phosphorylates spatially distinct targets to differentially regulate the kinetochore-microtubule interface. *Mol. Cell* **38**, 383-392.

Wigge, P. A. and Kilmartin, J. V. (2001). The Ndc80p complex from Saccharomyces cerevisiae contains conserved centromere components and has a function in chromosome segregation. *J. Cell Biol*. **152**, 349-360.

Yasui, Y., Urano, T., Kawajiri, A., Nagata, K., Tatsuka, M., Saya, H., Furukawa, K., Takahashi, T., Izawa, I. and Inagaki, M. (2004). Autophosphorylation of a newly identified site of Aurora-B is indispensable for cytokinesis. *J. Biol. Chem*. **279**, 12997-3003.

Zhai, Y., Kronebusch, P. J. and Borisy, G. G. (1995). Kinetochore microtubule dynamics and the metaphase-anaphase transition. *J. Cell Biol*. **131**, 721-734.

Journal of Cell Science